JACS
JOURNAL OF THE AMERICAN CHEMICAL SOCIETY

Communication

pubs.acs.org/JACS

Fast Photodriven Electron Spin Coherence Transfer: A Quantum Gate Based on a Spin Exchange *J*-Jump

Lukáš Kobr, Daniel M. Gardner, Amanda L. Smeigh, Scott M. Dyar, Steven D. Karlen, Raanan Carmieli, and Michael R. Wasielewski*

Department of Chemistry and Argonne–Northwestern Solar Energy Research (ANSER) Center, Northwestern University, Evanston, Illinois 60208-3113, United States

Supporting Information

ABSTRACT: Photoexcitation of the electron donor (D) within a linear, covalent donor–acceptor–acceptor molecule (D-A_1-A_2) in which A_1 = A_2 results in sub-nanosecond formation of a spin-coherent singlet radical ion pair state, $^1(D^{+\bullet}\text{-}A_1^{-\bullet}\text{-}A_2)$, for which the spin–spin exchange interaction is large: $2J$ = 79 ± 1 mT. Subsequent laser excitation of $A_1^{-\bullet}$ during the lifetime of $^1(D^{+\bullet}\text{-}A_1^{-\bullet}\text{-}A_2)$ rapidly produces $^1(D^{+\bullet}\text{-}A_1\text{-}A_2^{-\bullet})$, which abruptly decreases $2J$ 3600-fold. Subsequent coherent spin evolution mixes $^1(D^{+\bullet}\text{-}A_1\text{-}A_2^{-\bullet})$ with $^3(D^{+\bullet}\text{-}A_1\text{-}A_2^{-\bullet})$, resulting in mixed states which display transient spin-polarized EPR transitions characteristic of a spin-correlated radical ion pair. These photodriven *J*-jump experiments show that it is possible to use fast laser pulses to transfer electron spin coherence between organic radical ion pairs and observe the results using an essentially background-free time-resolved EPR experiment.

Controlling the spin dynamics of complex multispin molecular systems is a major goal in spintronics and quantum information processing.[1] Fast photoinitiated electron transfer within covalently linked organic donor–acceptor (D-A) molecules having specific D-A distances and orientations results in formation of spin-entangled electron–hole pairs (i.e., radical ion pairs, RPs) having well-defined initial spin configurations, while time-resolved electron paramagnetic resonance (TREPR) techniques provide an important means of manipulating and controlling these coherent spin states.[2] Organic RPs display coherent spin motion for up to ~100 ns,[3] which makes it possible that this coherence may provide the basis for new quantum information-processing strategies based on organic molecules.

We have previously demonstrated that RP populations within linear and branched D-A_1-A_2 arrays can be controlled using one wavelength-selective laser pulse to generate $D^{+\bullet}\text{-}A_1^{-\bullet}\text{-}A_2$ and a subsequent wavelength-selective laser pulse to excite $A_1^{-\bullet}$, resulting in the thermodynamically uphill reaction $D^{+\bullet}\text{-}A_1^{-\bullet}\text{-}A_2 \rightarrow D^{+\bullet}\text{-}A_1\text{-}A_2^{-\bullet}$.[4] Because of the close proximity of $D^{+\bullet}$ and $A_1^{-\bullet}$, exponentially distance-dependent Heisenberg spin–spin exchange coupling ($2J$) between $D^{+\bullet}$ and $A_1^{-\bullet}$ is necessarily large,[5] while that between $D^{+\bullet}$ and $A_2^{-\bullet}$ is much smaller. Here we show that laser excitation of the $A_1^{-\bullet}$ radical ion results in coherent transfer of the initial $D^{+\bullet}\text{-}A_1^{-\bullet}\text{-}A_2$ RP spin state to $D^{+\bullet}\text{-}A_1\text{-}A_2^{-\bullet}$.

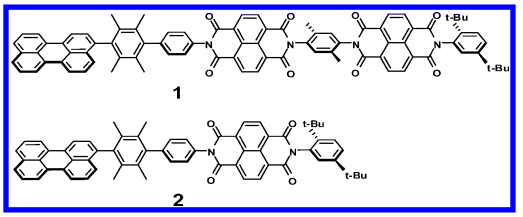

Syntheses of **1** and **2** are described in the Supporting Information. All synthetic intermediates and final products were characterized by ^{1}H and ^{13}C NMR, MALDI-TOF, MS-ESI, and UV–vis spectroscopy. Attachment of the 2,3,5,6-tetramethylbiphenyl group (B_1) to perylene (PER) in **1** and **2** shifts the 438 nm absorption maximum of PER in toluene slightly to 446 nm (Figure 1). This is consistent with the expected molecular

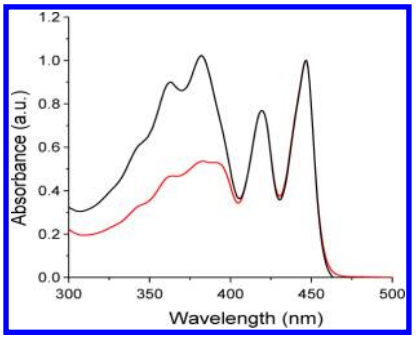

Figure 1. Normalized UV–vis spectra of **1** (black) and **2** (red) in toluene.

geometry, where the durene π system should be nearly orthogonal to that of PER due to steric effects of its methyl groups. Absorption spectra of both naphthalene-1,8:4,5-bis-(dicarboximide) (NDI) acceptors in **1** and the single NDI acceptor in **2** are not perturbed by their attachment to the 2,5-dimethylphenyl group (B_2).[6] Ground-state spectra of both **1** and **2** indicate that the electronic coupling between PER and NDI is weak.

Cyclic voltammetry on **1** and **2** at a Pt electrode in butyronitrile containing 0.1 M Bu_4NPF_6 (Figure S1A,B) shows two reversible one-electron NDI reduction waves at E_{red} = −0.53 and −1.02 V vs SCE,[6] and a single reversible one-electron PER oxidation wave at E_{ox} = 1.06 V vs SCE.[7] Reduction potentials of

Received: June 11, 2012

   dx.doi.org/10.1021/ja305650x | *J. Am. Chem. Soc.* XXXX, XXX, XXX–XXX

the two NDIs in **1** are indistinguishable; however, using differential pulse voltammetry (Figure S1C), the second reduction peak of **1** is somewhat asymmetric. The NDI reduction waves of **1** have about twice the current as the PER oxidation wave; they result from independent reduction of each NDI within **1**. Using the Weller equation (see Supporting Information), estimated energies of $PER^{+\bullet}$-B_1-$NDI_1^{-\bullet}$-B_2-NDI_2 and $PER^{+\bullet}$-B_1-$NDI_1^{-\bullet}$ for **1** and **2** in toluene are both 2.46 eV, while that of $PER^{+\bullet}$-B_1-NDI_1-B_2-$NDI_2^{-\bullet}$ for **1** is 2.62 eV. Since the ^{1}*PER energy is 2.76 eV, the free energies for photogenerating all RPs are favorable. However, the significantly longer RP distance of $PER^{+\bullet}$-B_1-NDI_1-B_2-$NDI_2^{-\bullet}$ (29.0 Å) relative to that of $PER^{+\bullet}$-B_1-$NDI_1^{-\bullet}$-B_2-NDI_2 (16.6 Å) results in an additional 0.16 eV Coulombic energy change, making electron transfer to NDI_2 energetically less favorable than that to NDI_1.

Transient absorption spectra of **1** in toluene at 295 K following selective photoexcitation of PER with a 416 nm, 120 fs laser pulse (Figure 2A) show initial formation of a strong ^{1}*PER absorption

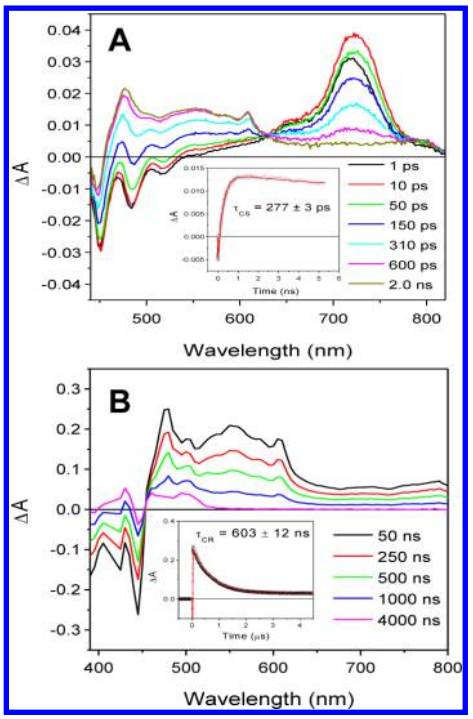

Figure 2. Transient absorption spectra of **1** in toluene at 295 K. (A) Following a 416 nm, 120 fs laser pulse. Inset: transient kinetics monitored at 520 nm. (B) Following a 416 nm, 7 ns laser pulse. Inset: transient kinetics monitored at 480 nm.

band at 720 nm,[8] which decays with the simultaneous appearance of a broad $PER^{+\bullet}$ absorption centered around 550 nm[9] and two $NDI^{-\bullet}$ absorption bands at 480 and 610 nm.[6] Charge separation (CS) kinetics are fit at 520 nm to a time constant of $\tau_{CS} = 277 \pm 3$ ps. Given that the ^{1}*PER lifetime is 4.6 ns,[10] the resultant quantum yield of charge separation is 94%. At later times, corresponding nanosecond transient absorption spectra (Figure 2B) show that the $PER^{+\bullet}$ and $NDI^{-\bullet}$ absorptions decay with a charge recombination (CR) time constant of $\tau_{CR} = 603 \pm 12$ ns. Residual long-lived absorption near 500 nm results from ^{3}*PER produced by CR in a 45% yield.[11] Corresponding data acquired for control dyad **2** (Figure S2A,B) give $\tau_{CS} = 300 \pm 3$ ps and $\tau_{CR} = 680 \pm 3$ ns. The similarity between the time constants for both charge separation and recombination in **1** and **2** indicates that 416 nm excitation produces only $PER^{+\bullet}$-B_1-$NDI_1^{-\bullet}$-B_2-NDI_2 in **1**, which is consistent with the fact that moving the electron from NDI_1 to NDI_2 requires a Coulomb energy penalty of 0.16 eV.

Rapid charge separation from the ^{1}*PER precursor state results in formation of the singlet RP: ^{1}($PER^{+\bullet}$-B_1-$NDI_1^{-\bullet}$-B_2-NDI_2), which may undergo electron−nuclear hyperfine coupling-induced radical pair intersystem crossing (RP-ISC) to produce the triplet RP, ^{3}($PER^{+\bullet}$-B_1-$NDI_1^{-\bullet}$-B_2-NDI_2). Subsequent CR is spin selective; i.e., the singlet RP recombines to the singlet ground state, and the triplet RP recombines to yield the neutral local triplet (Figure 3A). Application of a static magnetic

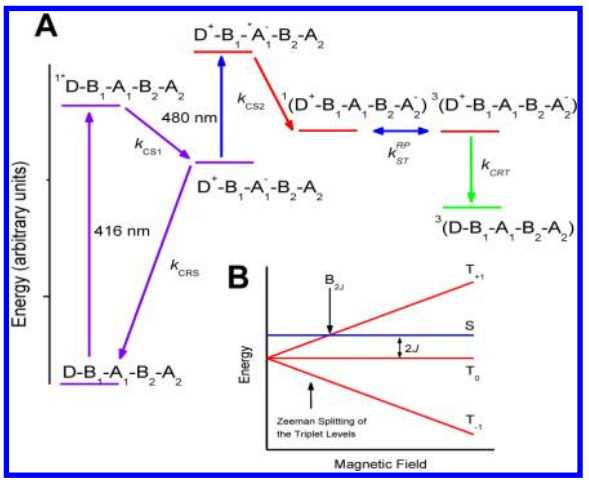

Figure 3. (A) Energy levels and electron-transfer pathways. D = PER, A = NDI. (B) Expanded view of the RP energy levels as a function of magnetic field ($2J > 0$).

field causes Zeeman splitting of the RP triplet sublevels, and varying the field strength modulates the efficiency of RP-ISC by adjusting the energies of the triplet sublevels relative to that of the singlet level (Figure 3B). When the Zeeman splitting of the triplet RP sublevels equals the intrinsic singlet−triplet splitting, $2J$, of the RP, there is an increase in RP-ISC rate. This increase translates into a maximum in triplet RP production and therefore a maximum in neutral local triplet yield upon CR. By monitoring the yield of local triplet production as a function of applied magnetic field, the magnitude of $2J$ can be measured directly.[12] $2J$ within $PER^{+\bullet}$-B_1-$NDI_1^{-\bullet}$-B_2-NDI_2 was measured using the effect of a magnetic field on the ^{3}*PER yield monitored at 480 nm and 4 μs following the laser pulse. The ^{3}*PER yield for **1** exhibits a resonance at $2J = 79 \pm 1$ mT (Figure 4), while a similar resonance is observed for **2** at $2J = 82 \pm 1$ mT (Figure S3). Similar $2J$ values

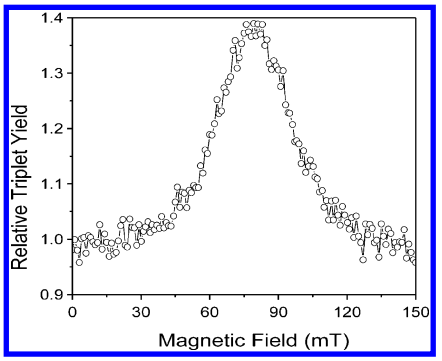

Figure 4. Relative triplet yield monitored at 480 nm as a function of magnetic field strength for **1** in toluene at 295 K following a 416 nm, 7 ns laser pulse.

dx.doi.org/10.1021/ja305650x | J. Am. Chem. Soc. XXXX, XXX, XXX−XXX

for **1** and **2** provide additional evidence that $PER^{+\bullet}$-B_1-$NDI_1^{-\bullet}$-B_2-NDI_2 is primarily populated within **1**. Since $2J$ depends exponentially on distance, moving the electron to NDI_2 should result in a large decrease in $2J$.

TREPR spectra were acquired using continuous microwave irradiation in a ~350 mT magnetic field (see Supporting Information), so that the Zeeman split triplet RP sublevels are best described by the T_{+1}, T_0, and T_{-1} eigenstates that are quantized along the applied magnetic field, while the singlet RP energy level (S) is unaffected (Figure 3B).[2b,d,13] RP-ISC depends on both the spin−spin exchange interaction ($2J$) and the dipolar interaction (D) between the two radicals that comprise RP. $2J$ depends exponentially on the distance (r) between the two radicals and is assumed to be isotropic, while D depends on $1/r^3$ and is anisotropic. In fluid solution, however, D is rotationally averaged to zero for small molecules such as **1** and **2**.

When $2J$ is large, such as the ~80 mT values observed for $PER^{+\bullet}$-B_1-$NDI_1^{-\bullet}$-B_2-NDI_2 and $PER^{+\bullet}$-B_1-$NDI_1^{-\bullet}$, S−T_0 mixing is generally weak.[14] However, when $2J$ is generally <10 mT, coherent S−T_0 mixing occurs,[2b,d,13] and the two resulting mixed states are preferentially populated due to the initial population of S, so that the four EPR transitions that occur between these mixed states and initially the unpopulated T_{+1} and T_{-1} states are spin polarized.[14a,15] The TREPR spectrum consists of two antiphase doublets, centered at the g-factors of the individual radicals that comprise the pair, in which splitting of each doublet is determined by $2J$. The electron spin polarization pattern from low field to high field of the EPR signal, i.e., which transitions are in enhanced absorption (a) or emission (e), is determined by the sign rule:[2d,16] $\Gamma = \mu\cdot\mathrm{sign}(2J) = (-)$ gives e/a or $= (+)$ gives a/e, where $\mu = -1$ or $+1$ for a singlet or triplet excited-state precursor, respectively. Thus, if $2J > 0$, singlet excited-state precursors yield an (e,a,e,a) line pattern. If the g-factors of the two radicals are similar and are split by hyperfine couplings, the two doublets overlap strongly and appear as a distorted (e,a) signal. The spectra are simulated by applying the spin-correlated radical pair model using $2J$ along with the g-factors and hyperfine coupling constants of $D^{+\bullet}$ and $A^{-\bullet}$.[14,15,17]

TREPR spectra of **1** and **2** in toluene at 295 K following selective 416-nm photoexcitation of PER show only a very weak signal for **1** (Figure 5) and no signal for **2**. This is consistent with the very large $2J$ value measured directly by the magnetic field effect on the ^{3}*PER yield. The large $2J$ value inhibits S−T_0 mixing, resulting in a greatly decreased transition probability between these states and $T_{\pm1}$.[2g,14,17b] The weak signal observed for **1** most likely results from generation of a small population of $NDI_2^{-\bullet}$ that is strongly spin-polarized.

Our previous results have shown that photoexcitation of $NDI^{-\bullet}$ at 480 nm produces its excited doublet state (^{2}*$NDI^{-\bullet}$) that has a 260 ps lifetime.[6] This lifetime is sufficiently long to allow electron transfer from ^{2}*$NDI^{-\bullet}$ to nearby electron acceptors.[4] The short-distance B_2 bridging molecule between two NDI molecules in **1** makes electron transfer from ^{2}*$NDI_1^{-\bullet}$ to NDI_2 kinetically favorable. In principle, fast electron transfer from $NDI_1^{-\bullet}$ to NDI_2 should not perturb the coherence of the two spins within the initial RP, but should transfer it intact to the second RP. Selective 416 nm photoexcitation of PER within **1** at $t = 0$ followed by selective 480 nm photoexcitation of $NDI_1^{-\bullet}$ at $t =$ 15 ns results in appearance of a strong spin-polarized RP signal (Figure 5). Irradiation of **1** and **2** with a single laser pulse at 480 nm, which is not absorbed by their ground states, does not result in any EPR signals (Figure S4). Simulation of experimental spin-polarized RP spectra using the model of Till and Hore[17b] yields

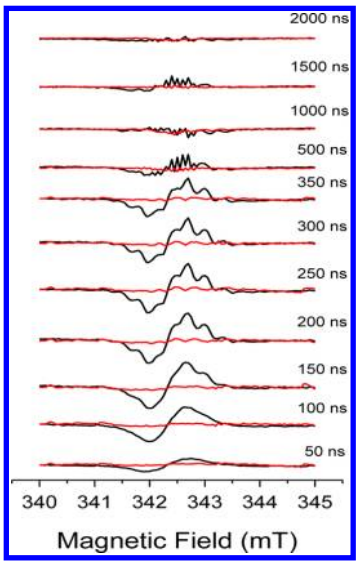

Figure 5. TREPR spectra of **1** in toluene at 295 K at indicated times following a single 416 nm, 7 ns laser pulse at $t_{416} = 0$ (red traces), and following the two-pulse sequence: 416 nm, 7 ns laser pulse at $t_{416} = 0$; 480 nm, 7 ns laser pulse at $t_{480} = 15$ ns (black traces).

$2J$ = 0.022 mT (Figure S5). Thus, rapid photodriven electron transfer from the initial RP to the secondary RP results in a nearly 3600-fold decrease in $2J$.

The spin-polarized RP signal that appears following photoexcitation of **1** with an initial 416 nm laser pulse at $t_{416} = 0$ and a second, subsequent 480 nm laser pulse at t_{480} shows an interesting dependence on $t_{480} - t_{416}$, the time delay between 416 and 480 nm laser pulses (Figure 6). Times of the laser pulses

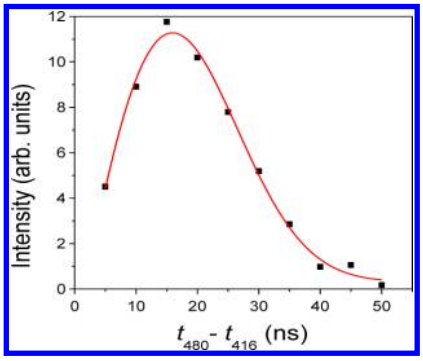

Figure 6. Intensity of the spin-polarized EPR signal of **1** in toluene at 295 K and 100 ns as a function of time delay, $t_{480} - t_{416}$, between the 416 nm, 7 ns laser pulse at $t_{416} = 0$ and the second 480 nm, 7 ns laser pulse at t_{480}.

are measured at the maximum intensity of each pulse. The data are fit to the convolution of a Gaussian function with a width of 10 ± 1 ns and a single-exponential decay of 11 ± 1 ns. Since the 416 and 480 nm laser pulse widths (fwhm) are both 7 ns, the slow rise of the spin-polarized RP EPR signal results from buildup of the initial $PER^{+\bullet}$-B_1-$NDI_1^{-\bullet}$-B_2-NDI_2 population during the 416 nm pulse convolved with electron transfer from $ND1_1^{-\bullet}$ to NDI_2 induced by the second 480 nm pulse. Rapid photogeneration of $PER^{+\bullet}$-B_1-$NDI_1^{-\bullet}$-B_2-NDI_2 using 416 nm excitation results in zero quantum coherence (ZQC) between the S and T_0 energy levels.[3c,17a,18] Rapid dephasing of ZQC results from the interaction of the electron spins with their environment, and only a very small amount of S−T_0 mixing occurs because $2J$ is

dx.doi.org/10.1021/ja305650x | J. Am. Chem. Soc. XXXX, XXX, XXX−XXX

large.[14] If the 480 nm pulse is applied prior to dephasing, then ZQC is transferred from $PER^{+\bullet}$-B_1-$NDI_1^{-\bullet}$-B_2-NDI_2 to $PER^{+\bullet}$-B_1-NDI_1-B_2-$NDI_2^{-\bullet}$, wherein abrupt reduction in $2J$ greatly increases $S-T_0$ mixing and the transition probability from the mixed states to $T_{\pm1}$, resulting in the appearance of spin-polarized EPR signal.[14] In contrast, when the 480 nm pulse is applied after dephasing in $PER^{+\bullet}$-B_1-$NDI_1^{-\bullet}$-B_2-NDI_2 is complete, $2J$ is still dramatically reduced, but coherent $S-T_0$ mixing does not occur. The small amount of $S-T_0$ mixing generated in $PER^{+\bullet}$-B_1-$NDI_1^{-\bullet}$-B_2-NDI_2 is insufficient to produce an observable spin-polarized EPR signal in $PER^{+\bullet}$-B_1-NDI_1-B_2-$NDI_2^{-\bullet}$. In fact, no spin-polarized EPR signal is observed when $t_{480} - t_{416} > 50$ ns. Thus, the observed 11 ± 1 ns decay time of the EPR signal most likely reflects the ZQC dephasing time of $PER^{+\bullet}$-B_1-$NDI_1^{-\bullet}$-B_2-NDI_2.

Our data illustrate how laser manipulation of coherent spin states can control magnetic interactions between spins, offering new opportunities to design molecular systems for studying quantum information processing.

■ ASSOCIATED CONTENT

Ⓢ Supporting Information

Experimental details including synthesis, electrochemistry, and additional transient optical and EPR data. This material is available free of charge via the Internet at http://pubs.acs.org.

■ AUTHOR INFORMATION

Corresponding Author

m-wasielewski@northwestern.edu

Notes

The authors declare no competing financial interest.

■ ACKNOWLEDGMENTS

The authors thank Dr. Oleg Poluektov (Argonne National Laboratory) for stimulating discussions. This work was supported by the National Science Foundation under Grant No. CHE-1012378. D.M.G. thanks the NDSEG for a graduate fellowship. A.L.S. and R.C. were supported as part of the ANSER Center, an Energy Frontier Research Center funded by the U.S. Department of Energy, Office of Science, Office of Basic Energy Sciences, under award no. DE-SC0001059.

■ REFERENCES

(1) (a) Gershenfeld, N. A.; Chuang, I. L. *Science* **1997**, *275*, 350. (b) Mehring, M. *Appl. Magn. Reson.* **1999**, *17*, 141. (c) Harneit, W. *Phys. Rev. A* **2002**, *65*, 032322. (d) Morton, J. J. L.; Tyryshkin, A. M.; Ardavan, A.; Porfyrakis, K.; Lyon, S. A.; Briggs, G. A. D. *Los Alamos National Laboratory, Preprint Archive, Quantum Physics* **2004**, 1. (e) Mehring, M.; Mende, J. *Phys. Rev. A: At., Mol., Opt. Phys.* **2006**, *73*, 052303/1. (f) Salikhov, K. M.; Golbeck, J. H.; Stehlik, D. *Appl. Magn. Reson.* **2007**, *31*, 237. (g) Sato, K.; Nakazawa, S.; Rahimi, R.; Ise, T.; Nishida, S.; Yoshino, T.; Mori, N.; Toyota, K.; Shiomi, D.; Yakiyama, Y.; Morita, Y.; Kitagawa, M.; Nakasuji, K.; Nakahara, M.; Hara, H.; Carl, P.; Hoefer, P.; Takui, T. *J. Mater. Chem.* **2009**, *19*, 3739. (h) Wesenberg, J. H.; Ardavan, A.; Briggs, G. A. D.; Morton, J. J. L.; Schoelkopf, R. J.; Schuster, D. I.; Molmer, K. *Phys. Rev. Lett.* **2009**, *103*, 070502/1. (i) Nakahara, M., Ota, Y., Rahimi, R., Kondo, Y., Tada-Umezaki, M., Eds. *Molecular Realizations of Quantum Computing 2007*; World Scientific Publishing: Singapore, 2009; Vol. 2. (j) Kandrashkin, Y. E.; Salikhov, K. M. *Appl. Magn. Reson.* **2010**, *37*, 549. (k) Morita, Y.; Yakiyama, Y.; Nakazawa, S.; Murata, T.; Ise, T.; Hashizume, D.; Shiomi, D.; Sato, K.; Kitagawa, M.; Nakasuji, K.; Takui, T. *J. Am. Chem. Soc.* **2010**, *132*, 6944. (l) Yoshino, T.; Nishida, S.; Sato, K.; Nakazawa, S.; Rahimi, R. D.; Toyota, K.; Shiomi, D.; Morita, Y.; Kitagawa, M.; Takui, T. *J. Phys. Chem. Lett.* **2011**, *2*, 449. (m) Brown, R. M.; Tyryshkin, A. M.; Porfyrakis, K.; Gauger, E. M.; Lovett, B. W.; Ardavan, A.; Lyon, S. A.; Briggs, G. A. D.; Morton, J. J. L. *Phys. Rev. Lett.* **2011**, *106*, 110504/1.

(2) (a) Hasharoni, K.; Levanon, H.; Greenfield, S. R.; Gosztola, D. J.; Svec, W. A.; Wasielewski, M. R. *J. Am. Chem. Soc.* **1995**, *117*, 8055. (b) Carbonera, D.; DiValentin, M.; Corvaja, C.; Agostini, G.; Giacometti, G.; Liddell, P. A.; Kuciauskas, D.; Moore, A. L.; Moore, T. A.; Gust, D. *J. Am. Chem. Soc.* **1998**, *120*, 4398. (c) Shaakov, S.; Galili, T.; Stavitski, E.; Levanon, H.; Lukas, A.; Wasielewski, M. R. *J. Am. Chem. Soc.* **2003**, *125*, 6563. (d) Dance, Z. E. X.; Mi, Q.; McCamant, D. W.; Ahrens, M. J.; Ratner, M. A.; Wasielewski, M. R. *J. Phys. Chem. B* **2006**, *110*, 25163. (e) Miura, T.; Carmieli, R.; Wasielewski, M. R. *J. Phys. Chem. A* **2010**, *114*, 5769. (f) Miura, T.; Scott, A. M.; Wasielewski, M. R. *J. Phys. Chem. C* **2010**, *114*, 20370. (g) Colvin, M. T.; Ricks, A. B.; Scott, A. M.; Smeigh, A. L.; Carmieli, R.; Miura, T.; Wasielewski, M. R. *J. Am. Chem. Soc.* **2011**, *133*, 1240. (h) Miura, T.; Wasielewski, M. R. *J. Am. Chem. Soc.* **2011**, *133*, 2844.

(3) (a) Kothe, G.; Weber, S.; Ohmes, E.; Thurnauer, M. C.; Norris, J. R. *J. Phys. Chem.* **1994**, *98*, 2706. (b) Laukenmann, K.; Weber, S.; Kothe, G.; Oesterle, C.; Angerhofer, A.; Wasielewski, M. R.; Svec, W. A.; Norris, J. R. *J. Phys. Chem.* **1995**, *99*, 4324. (c) Hoff, A. J.; Gast, P.; Dzuba, S. A.; Timmel, C. R.; Fursman, C. E.; Hore, P. J. *Spectrochim. Acta, Part A* **1998**, *54A*, 2283.

(4) (a) Debreczeny, M. P.; Svec, W. A.; Marsh, E. M.; Wasielewski, M. R. *J. Am. Chem. Soc.* **1996**, *118*, 8174. (b) Lukas, A. S.; Miller, S. E.; Wasielewski, M. R. *J. Phys. Chem. B* **2000**, *104*, 931. (c) Lukas, A. S.; Bushard, P. J.; Wasielewski, M. R. *J. Am. Chem. Soc.* **2001**, *123*, 2440.

(5) Heisenberg, W. *Z. Phys.* **1926**, *38*, 411.

(6) Gosztola, D.; Niemczyk, M. P.; Svec, W.; Lukas, A. S.; Wasielewski, M. R. *J. Phys. Chem. A* **2000**, *104*, 6545.

(7) Kubota, T.; Miyazaki, H.; Ezumi, K.; Yamakawa, M. *Bull. Chem. Soc. Jpn.* **1974**, *47*, 491.

(8) Pagès, S.; Lang, B.; Vauthey, E. *J. Phys. Chem. A* **2003**, *108*, 549.

(9) Shida, T. *Electronic Absorption Spectra of Radical Ions*; Elsevier: New York, 1988.

(10) Katoh, R.; Sinha, S.; Murata, S.; Tachiya, M. *J. Photochem. Photobiol. A* **2001**, *145*, 23.

(11) (a) Bensasson, R.; Land, E. J. *Trans. Faraday Soc.* **1971**, *67*, 1904. (b) Rachford, A. A.; Goeb, S.; Ziessel, R.; Castellano, F. N. *Inorg. Chem.* **2008**, *47*, 4348.

(12) (a) Anderson, P. W. *Phys. Rev.* **1959**, *115*, 2. (b) Shultz, D. A.; Fico, R. M., Jr.; Bodnar, S. H.; Kumar, R. K.; Vostrikova, K. E.; Kampf, J. W.; Boyle, P. D. *J. Am. Chem. Soc.* **2003**, *125*, 11761. (c) Scott, A. M.; Miura, T.; Ricks, A. B.; Dance, Z. E. X.; Giacobbe, E. M.; Colvin, M. T.; Wasielewski, M. R. *J. Am. Chem. Soc.* **2009**, *131*, 17655.

(13) (a) Hasharoni, K.; Levanon, H.; Greenfield, S. R.; Gosztola, D. J.; Svec, W. A.; Wasielewski, M. R. *J. Am. Chem. Soc.* **1996**, *118*, 10228. (b) Kobori, Y.; Yamauchi, S.; Akiyama, K.; Tero-Kubota, S.; Imahori, H.; Fukuzumi, S.; Norris, J. R., Jr. *Proc. Natl. Acad. Sci. U.S.A.* **2005**, *102*, 10017.

(14) (a) Closs, G. L.; Forbes, M. D. E.; Norris, J. R. *J. Phys. Chem.* **1987**, *91*, 3592. (b) Buckley, C. D.; Hunter, D. A.; Hore, P. J.; McLauchlan, K. A. *Chem. Phys. Lett.* **1987**, *135*, 307.

(15) Hore, P. J.; Hunter, D. A.; Mckie, C. D.; Hoff, A. J. *Chem. Phys. Lett.* **1987**, *137*, 495.

(16) Hore, P. J. In *Advanced EPR in Biology and Biochemistry*; Hoff, A. J., Ed.; Elsevier: Amsterdam, 1989; pp 405.

(17) (a) Norris, J. R.; Morris, A. L.; Thurnauer, M. C.; Tang, J. *J. Chem. Phys.* **1990**, *92*, 4239. (b) Till, U.; Hore, P. J. *Mol. Phys.* **1997**, *90*, 289.

(18) (a) Salikhov, K. M.; Bock, C. H.; Stehlik, D. *Appl. Magn. Reson.* **1990**, *1*, 195. (b) Bittl, R.; Kothe, G. *Chem. Phys. Lett.* **1991**, *177*, 547. (c) Zwanenburg, G.; Hore, P. J. *Chem. Phys. Lett.* **1993**, *203*, 65. (d) Kothe, G.; Weber, S.; Ohmes, E.; Thurnauer, M. C.; Norris, J. R. *J. Phys. Chem.* **1994**, *98*, 2706.